PALEONTOLOGY

Paleozoic ammonoid ecomorphometrics test ecospace availability as a driver of morphological diversification

Christopher D. Whalen[1]*, Pincelli M. Hull[1,2], Derek E. G. Briggs[1,2]

The early burst model suggests that disparity rises rapidly to fill empty ecospace following clade origination or in the aftermath of a mass extinction. Early bursts are considered common features of fossil data, but neontological studies have struggled to identify them. Furthermore, tests have proven difficult because factors besides ecology can drive changes in morphology. Here, we document the ecomorphometric evolution of the extinct Ammonoidea at 1-million-year resolution, from their origination in the Early Devonian (Emsian) to the Early Triassic (Induan), over ~156 million years. This time interval encompasses six global extinction events, including two of the Big Five, and incorporates multiple ammonoid radiations. However, we find no evidence for early bursts of ecomorphological disparity. This contradicts arguments that the temporal scope, or traits measured in genomic data, conceal evidence of early bursts. Rather, early bursts may be less prevalent in fossil data than is often assumed.

INTRODUCTION

Simpson's (*1*) early burst model predicts that clade disparity arises early in radiations. Simpson (*1*) hypothesized that species rapidly differentiate to fill distinct niches either because these were vacant or because the radiating clade is competitively superior, with the rate of increasing disparity declining as niches fill. These early bursts of disparity are often considered the norm in the fossil record [e.g., (*2*–*4*)], despite examples to the contrary [e.g., (*5*, *6*)]. Furthermore, molecular phylogenetic analyses have struggled to identify them [e.g., (*7*, *8*)]. This paradox has given rise to the suggestion that early bursts are trait- and scale-specific and restricted to those features most linked to macrohabitat, diet, and higher-level clade origination (*9*). We test this suggestion by examining ammonoid ecomorphometric evolution through the Paleozoic; if an early burst occurred, then rates of increasing disparity should exceed the predictions based on rates of diversification. Ammonoids are an ideal group for isolating the potential drivers of change in morphological disparity because of their continuous and abundant fossil record through several extinction events and quantifiable relationship between shell shape and ecology (*10*–*12*).

Ammonoids survived six Paleozoic mass extinctions including two of the Big Five: the end-Frasnian and end-Permian events. They are also known to exhibit large changes in species richness (i.e., boom-and-bust diversity dynamics): Postextinction taxa originate from a small number of survivors (*13*–*15*). This dynamic effectively creates a "clean slate" so that postextinction recovery resembles a de novo origination event. Here, we investigate global patterns of Paleozoic ammonoid diversification and extinction using shell measurements in 749 ammonoid species over ~156 million years of evolution at 1-million-year intervals. We use the convex hull area to track the occupation of ecomorphospace in a given time interval relative to a null model of ecomorphospace occupation. Our null model simulated the extent and dynamics of ecomorphospace occupation expected, given species richness and longevity, by randomly assigning (with replacement) real morphologies to the same number and stratigraphic distribution of species. After accounting for the null model, the residual variance in our ecomorphological metrics provides evidence of the extent of (and changes in) ecomorphological disparity independent of species richness. Some increase in disparity coupled to an increase in richness is the null expectation. Early bursts are thus evidenced by an increase in disparity in excess of that predicted by diversification or, in other words, residual ecomorphological metrics above the null expectation.

Residual convex hull area measures how completely ammonoids occupy ecomorphospace relative to the null expectation (the occupancy "range"). We consider disparity within the null 50% range to be indistinguishable from the null ecomorphological expectation given the number and stratigraphic distribution of species. We interpret ecomorphological metrics above the inner 50% range of the null during origination or a mass extinction recovery as indicative of an early burst radiation.

Ammonoid gross morphology can be characterized by just three shell parameters (*12*): umbilical exposure (*U*), overall inflation rate or thickness ratio (*Th*), and whorl expansion rate (*w*) (*16*). Westermann Morphospace (WM) is an Aitchison simplex of these shell parameters depicted as a ternary diagram, where shell shapes are plotted on the basis of the proportional contributions of *U*, *Th*, and *w* to the overall morphology (Fig. 1) (*16*). These parameters (or slightly modified versions of them) are commonly used to describe ammonoid disparity through time—typically with *w*-*U* and *w*-*Th* bivariate plots [e.g., (*17*–*21*)]. Zones within WM predict hypothetical swimming modalities (Fig. 1) because they reflect fundamental properties of shell hydrodynamics (*10*, *16*). High *w* values should correspond to oxyconic nektic swimmers, high *Th* values correspond to serpenticonic planktic drifters, high *U* values correspond to spheroconic and cadiconic planktic vertical migrants, and intermediate values (e.g., *Nautilus*) correspond to maneuverable eudemersal generalists (Fig. 1). Initial simulations of these shapes in currents are consistent with WM predictions (*22*), suggesting that the axes (i.e., *U*, *Th*, and *w*) correspond to ecomorphological niches delimited by bathymetry (pelagic versus demersal) and swimming velocity (nektic versus planktic).

Because WM uses data in a ternary morphospace, distances within WM are nonlinear, necessitating the transformation of coordinates into Cartesian space before distance calculations. Therefore,

[1]Department of Earth and Planetary Sciences, Yale University, 210 Whitney Ave., New Haven, CT 06511, USA. [2]Peabody Museum of Natural History, Yale University, 170 Whitney Ave., New Haven, CT 06511, USA.
*Corresponding author. Email: christopher.whalen@yale.edu

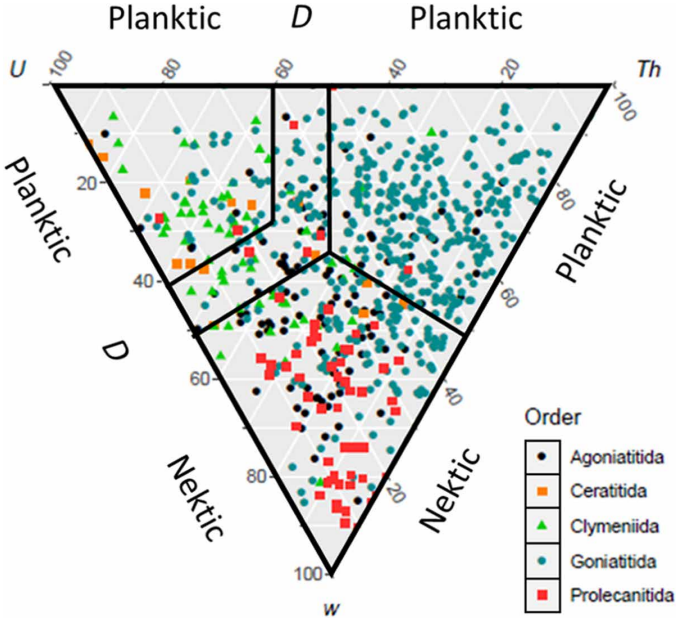

Fig. 1. Measured ammonoids in WM. *U*, umbilical exposure (maximized in serpenticones); *Th*, overall inflation (maximized in spherocones); *w*, whorl expansion (maximized in oxycones); *D*, demersal. Black lines demark areas for each ecomorphological megaguild.

we also constructed a principal components analysis (PCA) of the independent measurements used to generate WM coordinates to avoid warping morphospace distances amongst species. Principal component 2 (PC2; 25.4% of variance) correlates with *U* ($r = -0.799$), and PC3 (14.5% of variance) correlates with *Th* ($r = 0.760$); PC1 (58.7% of variance) does not correlate well with any WM axis (PC1 and *U*, $r = -0.275$; PC1 and *Th*, $r = 0.050$; PC1 and *w*, $r = 0.218$). Thus, PC2 and PC3 measure the ecologically relevant traits captured by WM through time and provide a measure of ecomorphological disparity that maintains relative distances in morphospace. This also suggests that more than half of the variance (i.e., PC1) observed in Paleozoic ammonoid shell morphology reflects something other than ecohydrodynamics. PC1 is most strongly affected by the whorl heights (fig. S4), which primarily factor into *w* in WM; however, conchal width is also a substantial factor in PC1 and not accounted for in calculating *w*. PC1 may record a phylogenetic signal, which could be useful for future investigations of the interrelationships of this clade, which exhibits high rates of convergent evolution (*23*).

RESULTS

During the late Silurian or Early Devonian, a group of orthoconic cephalopods (Bactritida) developed a curved shell (*24*), leading ultimately to the origin of Ammonoidea (*25*). The earliest Emsian ammonoids were open-coiled, but more hydrodynamic and maneuverable closed coils soon evolved and species richness rapidly increased (Fig. 2A) (*20*, *21*). Our metric of total ecomorphological disparity, the convex hull area of PC2 and PC3, captures this pattern of rapidly increasing absolute disparity throughout the Emsian (Fig. 2F, black line). However, early bursts should involve the accumulation of morphological disparity in excess of taxonomic richness, which is not the case here (Fig. 2G) and not just the rapid accumulation of morphological disparity accompanying clade diversification.

Corrected for species richness, the disparity of Emsian ammonoids contradicts expectations under an early burst model of trait evolution. The disparity of Emsian ammonoids only briefly exceeded the null expectation at 400 Ma, 6 million years after origination (Fig. 2, F and G). Excepting this and a 1-million-year anomaly at the base of the Givetian, the range of ammonoid ecomorphologies is well within, and at times below, null predictions for the first ~39 million years of their history (Fig. 2, F and G). The anomalously high residual disparity in the earliest Givetian (Fig. 2G) reflects the overlap of three species with extreme ecomorphologies: the last appearance of the oxyconic *Exopinacites singularis* and *Pinacites jugleri* and the first appearance of the serpenticonic *Tamarites subitus* (see the Supplementary Materials); this anomaly is not observed among mean pairwise distances (Fig. 2E).

For each of the six extinction events considered, ammonoid richness recovery is accomplished within 1 million years (Fig. 3A). There was no early burst of ammonoids following the end-Frasnian event (the Late Devonian mass extinction, one of the Big Five). Instead, during this richness recovery, residual disparity was lower than at any other time in the Paleozoic, dropping below the null 90% range (Fig. 2G). The most marked increase in disparity occurs in the mid-Famennian when there is a major taxonomic turnover (Fig. 2, B and C) and increase in species richness (Fig. 2A). This is the largest single increase in observed ecomorphological disparity (Fig. 2, E to G), but it is not associated with the origin of the clade or a mass extinction event (it occurs 8 million years after the end-Frasnian), contrary to expectations. During the Emsian to early Famennian, ammonoids were biased toward more streamlined (nektic) forms (Fig. 2D; i.e., proportionally more nekton), and the richness of planktic ammonoids was relatively low. During this interval, the macroplankton was instead dominated by orthocerid nautiloids (~28 to 55% of genera) and tentaculitoids (~15 to 31% of genera) (*26*). Thus, competitive exclusion may have played a role in preventing ammonoids from more fully exploiting planktic niches earlier (Fig. 2D). Tentaculitoids declined throughout the Devonian (*27*, *28*) and were among the groups hardest hit by the end-Frasnian extinction (*29*). This decline in other macroplankton may have created an opportunity for an increase in ammonoid ecomorphologies: Planktic ammonoid richness increased more than ninefold in the Famennian to account for ~71% of all macroplanktic genera (*26*).

Although richness increased through much of the Tournaisian (Fig. 2A), as with the other recoveries, the richness recovery from the end-Famennian only lasted 1 million years (Fig. 3A). During this time, disparity remained within null expectations (Fig. 2, F and G). Exceptionally high disparity is not observed until the mid-Tournaisian, from ~356 to 349 Ma, 4 million years after the end-Famennian (Fig. 2, E to G). The Tournaisian is the youngest Paleozoic stage characterized by high residual disparity (Fig. 2G). The recoveries associated with the Serpukhovian, end-Guadalupian, and end-Permian extinctions were all below null expectations (Fig. 2, F and G).

Ecologically selective extinction events are expected to result in a decrease in the occupation of ecomorphospace below the null 50% range as entire ecological modes are eliminated (*4*). Conversely, ecologically nonselective extinctions should result in ecomorphospace occupation consistent with that predicted by the loss of richness, because random attrition will tend, on average, to increase pairwise distances among surviving taxa while maintaining the mean pairwise distance (*4*). Ecomorphospace occupation above the null 50% range would indicate divergent selection as increased competition creates

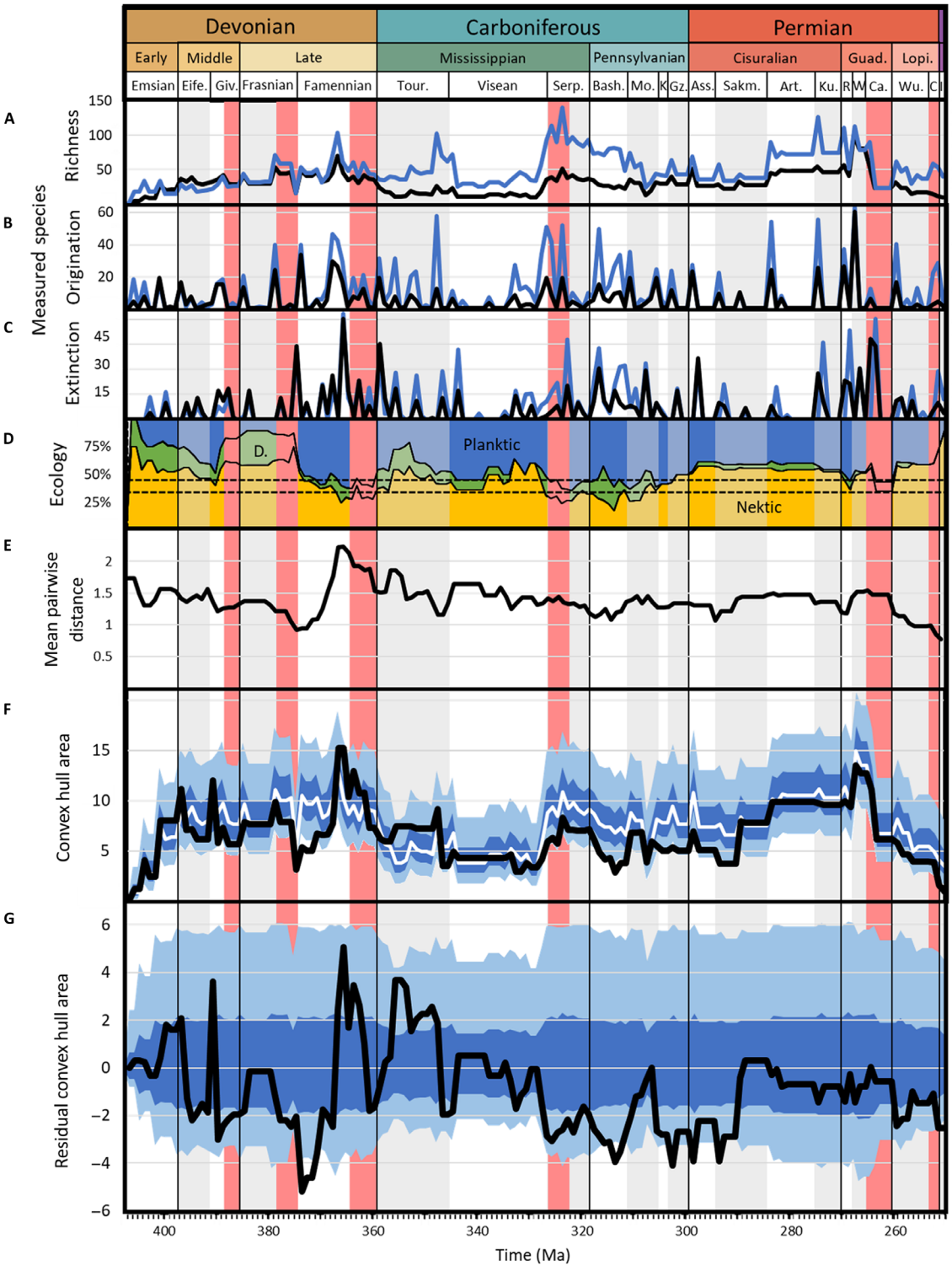

Fig. 2. Paleozoic ammonoid richness and disparity. Ranged-through (RT), per-million-year plots of ammonoid data from the Devonian (Emsian) through the Triassic (Induan). Purple, Triassic (Early Triassic); Guad., Guadalupian; Lopi., Lopingian; Eife., Eifelian; Giv., Givetian; Tour., Tournaisian; Serp., Serpukhovian; Bash., Bashkirian; Mo., Moscovian; K., Kasimovian; Gz., Gzhelian; Ass., Asselian; Sakm., Sakmarian; Art., Artinskian; Ku., Kungurian; R., Roadian; W., Wordian; Ca., Capitanian; Wu., Wuchiapingian; C., Changhsingian; I., Induan. Light red columns demark global mass extinction intervals (*43*). (**A** to **C**) Left axis and black lines, measured species; right axis and blue lines, total species in the AMMON database. (A) Species richness. (B) Species origination rates. (C) Species extinction rates. (**D**) Proportional ecomorphologies in WM; green, D., demersal; dashed line indicates relative area of each ecomorphological zone within WM; top, planktic; middle, demersal; bottom, nektic. (**E** to **G**) Disparity through time from PC2 and PC3. (E) Mean pairwise distances. (F to G) Dark blue shading, null 50% range; light blue shading, null 90% range. (F) Convex hull area; white line, null prediction. (G) Residual convex hull area.

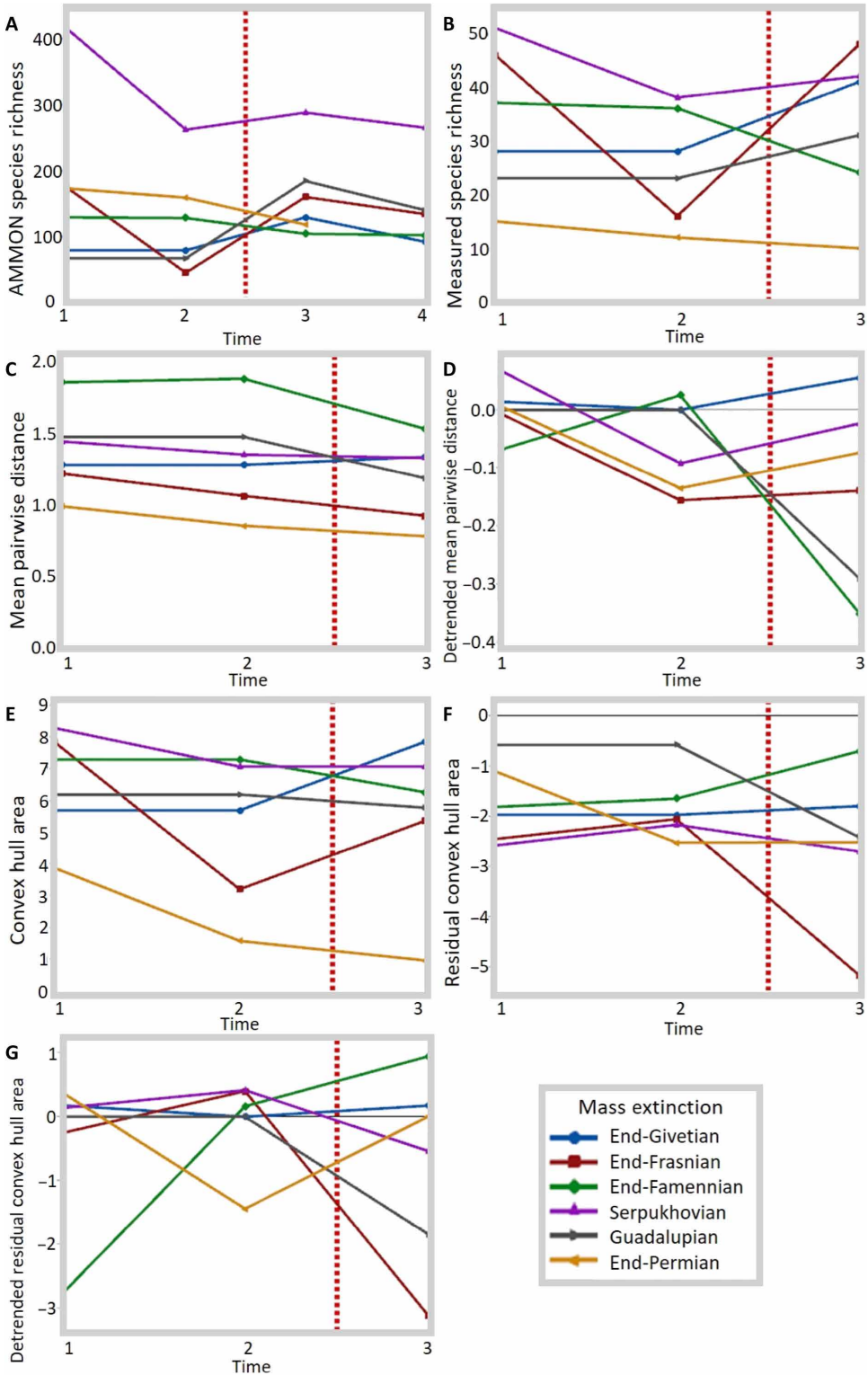

Fig. 3. Ammonoid mass extinction recoveries. Points, measured 1-million-year stratigraphic bins; vertical red dashed lines, mass extinction terminations; other lines: blue, end-Givetian; red, end-Frasnian; green, end-Famennian; purple, Serpukhovian; gray, end-Guadalupian; yellow, end-Permian. (**A**) Total ammonoid species richness from the AMMON database, showing the final 2 million years of each mass extinction and the following 2 million years. (**B** to **G**) Showing the final 2 million years of each mass extinction and the following 1 million years. (B) Measured ammonoid richness. (C) Mean pairwise distance. (D) Detrended mean pairwise distance. (E) Convex hull area. (F) Residual convex hull area. (G) Detrended residual convex hull area.

a low tolerance for similar ecological modes, or it may be a result of selective extinction of intermediates. By this measure, the end-Famennian, Serpukhovian, and end-Guadalupian extinctions were nonselective for ammonoid ecomorphology (Fig. 2). During the end-Frasnian and end-Permian events, the two Big Five mass extinctions, ammonoid ecomorphological disparity fell below the null 50% bound (Fig. 2, F and G); therefore, these mass extinctions appear to have been ecomorphologically selective. These results contradict the suggestion that both the end-Frasnian and end-Permian events were ecomorphologically nonselective for ammonoids and the end-Guadalupian mass extinction was selective for ammonoids (*20*). None of the six mass extinctions analyzed show signs of possible divergent selection with respect to ammonoid ecomorphology (Fig. 2, F and G).

The end-Frasnian and end-Permian extinctions are not followed by a burst of ecomorphological diversification. Species richness rapidly recovers from the end-Frasnian mass extinction (Fig. 2, A and C), but this pulse of speciation is coincident with a contraction in residual ecomorphospace (Fig. 2G). Demersal forms are largely absent from the species richness recovery (Fig. 2D), and this decline in ecospace occupation is reflected in a decline in disparity relative to the preceding Frasnian (Fig. 2, F and G). This loss of demersals may reflect the collapse of one of the most extensive global reef systems in Earth history during the end-Frasnian mass extinction (*30*, *31*), thereby selecting for survivors and postextinction species in a relatively limited number of ecomorphologies. Across marine metazoans, the end-Permian mass extinction is characterized by selectivity by biogeography, depth habitat (*32*), and physiology (*33*). Our evidence for a highly selective end-Permian event brings ammonoids in line with observations of other groups.

Mass extinctions are generally considered to open up ecospace by removing ecological incumbents, thereby allowing ecological (and morphological) innovation in their aftermath. The ecomorphological dynamics of ammonoids show that patterns of extinction and recovery may be much more complex and varied. In the aftermath of mass extinctions, ammonoid disparity is consistently within or below null predictions. Our residual disparity results (Fig. 2G) provide no support for early bursts of ecomorphology following mass extinctions as a driver of ammonoid ecomorphological innovation and expansion during the Paleozoic. Likewise, mean pairwise distances provide no support for early bursts (Fig. 2E). Disparity rarely exceeded the null 50% range and never exceeded the null 90% range (Fig. 2, F and G). Instead, disparity was often below the null 50% range and occasionally below the null 90% range (i.e., the early-Famennian; Fig. 2, F and G). This suggests that the majority of Paleozoic ammonoid species-level ecomorphological disparity can be explained by species richness alone, contrary to previous work (*20*).

DISCUSSION

A paradox of macroevolutionary theory is the apparent plethora of early bursts in the fossil record [e.g., (*2*, *3*, *34*, *35*)] but their rarity in neontological data [e.g., (*7*, *8*, *36*)]. This prompted the suggestion that early bursts are specific to ecologically relevant traits over long macroevolutionary time scales (*9*). Ammonoids are ideally situated to capture evidence of early bursts on the basis of these criteria because the long-lived clade is characterized by the convergent (and iterative) evolution of ecomorphologically distinct forms (*21*, *26*). However, our analysis finds no early burst during the Paleozoic. It does not follow that early bursts never occur in any metazoan group, but we think it is unlikely, on the basis of our findings, that they would be the norm. This result is unexpected as early bursts have been suggested in the context of the fossil record so frequently, as to be considered one of the few macroevolutionary rules (*2*).

One possible explanation for this discrepancy is our use of continuous trait data. Most studies of large-scale disparity patterns are based on discrete character-taxon matrices [e.g., (*2*, *3*)]. However, previous studies have found no substantial difference in the disparity profiles obtained independently from continuous measurements and from discrete character-taxon matrices (*37*, *38*). Therefore, continuous and discrete disparity measurements should yield the same results (*37*), and this is unlikely to explain our findings. Alternatively, early ecomorphological bursts may occur in the unknown soft tissue morphology of Paleozoic ammonoids, instead of the shell parameters investigated here, but it is unlikely that this would override the impact of shell shape on fundamental hydrodynamics and its ecological influence. Last, it is possible that early bursts are only evident in ammonoid subclades, rather than ammonoids as a whole, as in echinoids (*5*). Unfortunately, this is not testable given the high number of paraphyletic taxa (*39*, *40*) and absence of adequate phylogenies. However, early bursts should still be evident, were they to occur at the origin of Ammonoidea or during mass extinction recoveries when few clades survive or originate. Thus, our results provide strong evidence against any Paleozoic ammonoid early burst, challenging the generality of the early burst model in the fossil record.

No early burst was identified following the origination of ammonoids nor during their recovery from any Paleozoic mass extinction. High residual disparity is only observed during five intervals: briefly in the late Emsian, in the earliest Givetian (an apparent anomaly resulting from the overlap of three extreme morphologies), in the mid-Famennian, and twice in the mid-Tournaisian (Fig. 2G). None of these instances coincide with extinction recoveries. Our findings emphasize the importance of accounting for richness in comparing rates and mechanisms of morphological evolution. Ecomorphological disparity is dependent on species richness, so an early burst in ecomorphology must exceed the null expectation given the concomitant increase in species richness. The increase in disparity during the end-Frasnian recovery, for example, is actually slower than expected, given the increase in species richness. Thus, in terms of potential ecomorphological breadth, one of the most diverse, abundant, widespread, and long-ranging extinct groups shows no evidence of early bursts during the Paleozoic. As the stratigraphic resolution of other fossil taxa improves, similar studies may also find little support for the early burst model.

MATERIALS AND METHODS

We measured the whorl width (b), conch diameter (D), umbilical diameter (u), final whorl height (a), and 180° whorl height (a') of mature specimens of 749 Paleozoic-Induan ammonoid species; the larger conch radius (d) was also recorded since it is a commonly reported ammonoid measurement, but it is not used in any of our calculations (data file S1). These measurements were used to calculate the umbilical exposure (U'), overall inflation rate (Th'), and whorl expansion rate (w'), which were converted into U%, Th%, and w% coordinates in WM (*16*). All measurements, WM calculations, and

references can be found in the Supplementary Materials. The WM ternary diagram (Fig. 1) was created using the R package ggtern (*41*). We constructed the PCA in Minitab 19.1 using the *u*, *b*, *a*, and *a*′ measurements (*D* was excluded since $D = u + a + a'$).

$$U' = \frac{u/D}{0.52} \quad Th' = \frac{(b/D) - 0.14}{0.54} \quad w' = \frac{(a/a') - 1}{0.77}$$

$$U\% = \frac{U'}{U' + Th' + w'} \quad Th\% = \frac{Th'}{U' + Th' + w'} \quad w\% = \frac{w'}{U' + Th' + w'}$$

Stratigraphic ranges of all measured ammonoids were obtained from the AMMON online database (*42*) and resolved to 1-million-year chronostratigraphic bins. AMMON uses the geological time scale of Gradstein *et al.* (*43*), which is retained here despite revisions. Mass extinction intervals follow Bambach (*44*), which also uses Gradstein *et al.* (*43*). We used a ranged-through (RT) richness count to maximize samples per bin and because there is essentially no difference between the RT and sampled-in-bin counts of these data. We ensured that, once corrected for temporal autocorrelation, richness of measured ammonoid species per million year correlated with total ammonoid species richness per million year in AMMON ($R^2 = 71.65\%$; figs. S1 to S3).

WM is a ternary visualization of an Aitchison simplex (*45*); it must be transformed into Cartesian space before distance calculations (i.e., convex hull area). For this, we used the centered log ratio transform as implemented by the R package compositions (*46*). For each 1-million-year bin, we determined the area of the convex hull containing all species (for WM, PC1-PC2, and PC2-PC3) and the mean pairwise distance among all species (PC2 and PC3). All these calculations were performed in R 3.5.2, using code from the sp package (*47*).

We built a null model of ammonoid disparity through time by generating 10,000 bootstrap replicates of measured ammonoid PCs and Westermann coordinates (WCs) for each measured species. The total number of species and their stratigraphic ranges were unchanged; only PCs and WCs were resampled and randomly assigned to "species" (i.e., the stratigraphic ranges of the empirical dataset). The goal of this null model is to control for both the variation in richness and the temporal autocorrelation inherent in the empirical dataset. For each replicate, we calculated the convex hull area for each time bin of PC2 and PC3 (the dominant ecomorphologically relevant axes). For each 1-million-year chronostratigraphic bin, the median, 25th percentile, 75th percentile, 5th percentile, and 95th percentile of the 10,000 bootstrap replicates were recorded. The residual convex hull area for each 1-million-year bin was calculated for each metric by subtracting the observed metric (convex hull area of PC2 and PC3) from the median null model value.

Ammonoidea is monophyletic, but nearly all ammonoid orders (e.g., Agoniatitida, Goniatitida, and Prolecanitida) are paraphyletic (*15*, *39*). Thus, we treated Ammonoidea as a whole.

SUPPLEMENTARY MATERIALS

Supplementary material for this article is available at http://advances.sciencemag.org/cgi/content/full/6/37/eabc2365/DC1

View/request a protocol for this paper from *Bio-protocol*.

REFERENCES AND NOTES

1. G. G. Simpson, *Tempo and Mode in Evolution* (Columbia Univ. Press, 1944).
2. M. Hughes, S. Gerber, M. A. Wills, Clades reach highest morphological disparity early in their evolution. *Proc. Natl. Acad. Sci. U.S.A.* **110**, 13875–13879 (2013).
3. M. Foote, Morphological disparity in Ordovician-Devonian crinoids and the early saturation of morphological space. *Paleobiology* **20**, 320–344 (1994).
4. M. Foote, The evolution of morphological diversity. *Annu. Rev. Ecol. Syst.* **28**, 129–152 (1997).
5. M. J. Hopkins, A. B. Smith, Dynamic evolutionary change in post-Paleozoic echinoids and the importance of scale when interpreting changes in rates of evolution. *Proc. Natl. Acad. Sci. U.S.A.* **112**, 3758–3763 (2015).
6. J. L. Cantalapiedra, J. L. Prado, M. Hernández Fernández, M. T. Alberdi, Decoupled ecomorphological evolution and diversification in Neogene-Quaternary horses. *Science* **355**, 627–630 (2017).
7. M. N. Puttick, Mixed evidence for early bursts of morphological evolution in extant clades. *J. Evol. Biol.* **31**, 502–515 (2018).
8. L. J. Harmon, J. B. Losos, T. J. Davies, R. G. Gillespie, J. L. Gittleman, W. B. Jennings, K. H. Kozak, M. A. McPeek, F. Moreno-Roark, T. J. Near, A. Purvis, R. E. Ricklefs, D. Schluter, J. A. Schulte II, O. Seehausen, B. L. Sidlauskas, O. Torres-Carvajal, J. T. Weir, A. Ø. Mooers, Early bursts of body size and shape evolution are rare in comparative data. *Evolution* **64**, 2385–2396 (2010).
9. G. J. Slater, A. R. Friscia, Hierarchy in adaptive radiation: A case study using the Carnivora (Mammalia). *Evolution* **73**, 524–539 (2019).
10. G. E. G. Westermann, Ammonoid life and habitat, in *Ammonoid Paleobiology*, N. H. Landman, K. Tanabe, R. A. Davis, Eds. (Topics in Geobiology, Springer Science+Business Media, 1996), vol. 13, pp. 607–707.
11. G. E. G. Westermann, C. J. Tsujita, Life habits of ammonoids, in *Functional Morphology of the Invertebrate Skeleton* (John Wiley & Sons Ltd., 1999), pp. 299–325.
12. D. M. Raup, Geometric analysis of shell coiling: Coiling in ammonoids. *J. Paleo.* **41**, 43–65 (1967).
13. A. Brayard, G. Escarguel, H. Bucher, C. Monnet, T. Brühwiler, N. Goudemand, T. Galfetti, J. Guex, Good genes and good luck: Ammonoid diversity and the end-Permian mass extinction. *Science* **325**, 1118–1121 (2009).
14. S. M. Stanley, Evidence from ammonoids and conodonts for multiple Early Triassic mass extinctions. *Proc. Natl. Acad. Sci. U.S.A.* **106**, 15264–15267 (2009).
15. M. R. House, On the origin, classification and evolution of the early Ammonoidea, in *The Ammonoidea*, *Systematics Association Special Volume*, M. R. House, J. Senior, Eds. (Academic Press, 1981), vol. 18, pp. 3–36.
16. K. A. Ritterbush, D. J. Bottjer, Westermann Morphospace displays ammonoid shell shape and hypothetical paleoecology. *Paleobiology* **38**, 424–446 (2012).
17. W. B. Saunders, A. R. H. Swan, Morphology and morphologic diversity of mid-Carboniferous (Namurian) ammonoids in time and space. *Paleobiology* **10**, 195–228 (1984).
18. D. Korn, Morphospace occupation of ammonoids over the Devonian-Carboniferous boundary. *Paläont. Z.* **74**, 247–257 (2000).
19. D. Korn, C. Klug, Morphological pathways in the evolution of Early and Middle Devonian ammonoids. *Paleobiology* **29**, 329–348 (2003).
20. D. Korn, C. Klug, Palaeozoic ammonoids – diversity and development of conch morphology, in *Earth and Life: Global Biodiversity, Extinction Intervals and Biogeographic Perturbations Through Time*, J. A. Talent, Ed. (International Year of Planet Earth, Springer Science+Business Media, 2012), pp. 491–534.
21. W. B. Saunders, D. M. Work, S. V. Nikolaeva, The evolutionary history of shell geometry in Paleozoic ammonoids. *Paleobiology* **30**, 19–43 (2004).
22. K. A. Ritterbush, Interpreting drag consequences of ammonoid shells by comparing studies in Westermann Morphospace. *Swiss J. Palaeontol.* **135**, 125–138 (2016).
23. A. Tendler, A. Mayo, U. Alon, Evolutionary tradeoffs, Pareto optimality and the morphology of ammonite shells. *BMC Syst. Biol.* **9**, 12 (2015).
24. B. Kröger, R. H. Mapes, On the origin of bactritoids (Cephalopoda). *Paläontol. Z.* **81**, 316–327 (2007).
25. C. Klug, B. Kröger, J. Vinther, D. Fuchs, K. De Baets, Ancestry, origin and early evolution of ammonoids, in *Ammonoid Paleobiology: From Macroevolution to Paleogeography*, C. Klug, D. Korn, K. De Baets, I. Kruta, R. H. Mapes, Eds. (Springer, 2015), pp. 3–24.
26. C. D. Whalen, D. E. G. Briggs, The Palaeozoic colonization of the water column and the rise of global nekton. *Proc. R. Soc. B* **285**, 20180883 (2018).
27. J. M. Wittmer, A. I. Miller, Dissecting the global diversity trajectory of an enigmatic group: The paleogeographic history of tentaculitoids. *Palaeogeogr. Palaeoclimatol. Palaeoecol.* **312**, 54–65 (2011).
28. F. Wei, Y. Gong, H. Yang, Biogeography, ecology and extinction of Silurian and Devonian tentaculitoids. *Palaeogeogr. Palaeoclimatol. Palaeoecol.* **358–360**, 40–50 (2012).
29. D. Bond, The fate of the homoctenids (Tentaculitoidea) during the Frasnian–Famennian mass extinction (Late Devonian). *Geobiology* **4**, 167–177 (2006).
30. P. Copper, Reef development at the Frasnian/Famennian mass extinction boundary. *Palaeogeogr. Palaeoclimatol. Palaeoecol.* **181**, 27–65 (2002).

31. W. Kiessling, Geologic and biologic controls on the evolution of reefs. *Annu. Rev. Ecol. Evol. Syst.* **40**, 173–192 (2009).
32. J. L. Penn, C. Deutsch, J. L. Payne, E. A. Sperling, Temperature-dependent hypoxia explains biogeography and severity of end-Permian marine mass extinction. *Science* **362**, eaat1327 (2018).
33. A. H. Knoll, R. K. Bambach, J. L. Payne, S. Pruss, W. W. Fischer, Paleophysiology and end-Permian mass extinction. *Earth Planet. Sci. Lett.* **256**, 295–313 (2007).
34. R. B. J. Benson, N. E. Campione, M. T. Carrano, P. D. Mannion, C. Sullivan, P. Upchurch, D. C. Evans, Rates of dinosaur body mass evolution indicate 170 million years of sustained ecological innovation on the avian stem lineage. *PLOS Biol.* **12**, e1001853 (2014).
35. N. J. Minter, L. A. Buatois, M. G. Mángano, N. S. Davies, M. R. Gibling, R. B. MacNaughton, C. C. Labandeira, Early bursts of diversification defined the faunal colonization of land. *Nat. Ecol. Evol.* **1**, 0175 (2017).
36. T. Ingram, L. J. Harmon, J. B. Shurin, When should we expect early bursts of trait evolution in comparative data? Predictions from an evolutionary food web model. *J. Evol. Biol.* **25**, 1902–1910 (2012).
37. M. Romano, N. Brocklehurst, J. Fröbisch, Discrete and continuous character-based disparity analyses converge to the same macroevolutionary signal: A case study from captorhinids. *Sci. Rep.* **7**, 17531 (2017).
38. M. J. Hopkins, How well does a part represent the whole? A comparison of cranidial shape evolution with exoskeletal character evolution in the trilobite family Pterocephaliidae. *Palaeontology* **60**, 309–318 (2017).
39. A. J. McGowan, A. B. Smith, Ammonoids across the Permian/Triassic boundary: A cladistic perspective. *Palaeontology* **50**, 573–590 (2007).
40. D. Korn, Morphometric evolution and phylogeny of Palaeozoic ammonoids. Early and Middle Devonian. *Acta Geol. Pol.* **51**, 193–215 (2001).
41. N. Hamilton, ggtern. R Package version 3.3.0 (2018).
42. D. Korn, A. Ilg, AMMON (2007); www.wahre-staerke.com/ammon/.
43. F. M. Gradstein, J. G. Ogg, A. G. Smith, Eds., *A Geologic Time Scale 2004* (Cambridge Univ. Press, 2004).
44. R. K. Bambach, Phanerozoic biodiversity mass extinctions. *Annu. Rev. Earth Planet. Sci.* **34**, 127–155 (2006).
45. J. Aitchison, The statistical analysis of compositional data. *J. R. Stat. Soc. B.* **44**, 139–177 (1982).
46. K. G. van den Boogaart, compositions. R Package version 1.40-5 (2020).
47. E. Pebesma, R. Bivand, B. Rowlingson, V. Gomez-Rubio, R. J. Hijmans, M. Sumner, D. MacQueen, J. Lemon, J. O'Brien, J. O'Rourke, sp. R Package version 1.4-1 (2019).

Acknowledgments: We thank N. Mongiardino-Koch, D. Polly, J. Gauthier, B.-A. Bhullar, S. Westacott, and K. Ritterbush for useful conversations and advice; S. Butts and J. Utrup for specimen access and support; and M. Foote and M. Hopkins for insightful reviews of the submitted paper. **Funding:** C.D.W. was supported by Yale University; a travel grant from the Yale Graduate Student Assembly funded a conference presentation. **Author contributions:** C.D.W. and D.E.G.B. conceived of the study. C.D.W. collected all measurements and performed all calculations. The null model was devised by C.D.W. and P.M.H. All authors assisted in analyzing the data. C.D.W. prepared the manuscript with input from D.E.G.B. and P.M.H. C.D.W. created all figures. All authors edited and approved of the final manuscript. **Competing interests:** The authors declare that they have no competing interests. **Data and materials availability:** All data needed to evaluate the conclusions in the paper are present in the paper and the Supplementary Materials. Additional data related to this paper may be requested from the authors.

Submitted 14 April 2020
Accepted 21 July 2020
Published 9 September 2020
10.1126/sciadv.abc2365

Citation: C. D. Whalen, P. M. Hull, D. E. G. Briggs, Paleozoic ammonoid ecomorphometrics test ecospace availability as a driver of morphological diversification. *Sci. Adv.* **6**, eabc2365 (2020).